

Kagome Project: Physical and Numerical Modeling Comparison for a Post-formed Elastic Gridshell

Marc Leyral¹, Quentin Chef^{2,3}, Tom Bardout², Romain Antigny² and Alexis Meyer³

1. AMP Research Unit & Laboratory MAP-MAACC, ENSA Paris-La Villette, 144 Avenue de Flandre, Paris 75019, France

2. ENSA Paris-La Villette, Paris 75019, France

3. École Centrale-Supélec, Gif-sur-Yvette 91190, France

Featured Application: This study focuses on the evaluation of the critical buckling load for elastic gridshells by testing scale models or using dynamic relaxation. After discussing the differences between numerical and physical results at various scales, the study proposes to evaluate the resistance of certain gridshell typologies that cannot be reached numerically. The results can be used to design building covers or 1:1 pavilions made of elastic gridshells.

Abstract: An elastic gridshell is an efficient constructive typology for crossing large spans with little material. A flat elastic grid is built before buckling the structure into shape, in active and post-formed bending. The design and structural analysis of such a structure requires a stage of form finding that can mainly be done: (1) With a physical model: either by a suspended net method, or an active bending model; (2) With a numerical model performed by dynamic relaxation. All these solutions have various biases and assumptions that make them reflect more or less the reality. These three methods have been applied by Happold and Liddell [1] during the design of the Frei Otto's Mannheim Gridshell which has allowed us to compare the results, and to highlight the significant differences between digital and physical models. Based on our own algorithm called ELASTICA [2], our study focuses on: (1) Comparing the results of the ELASTICA's numerical models to load tests on physical models; (2) The identification of the various factors that can influence the results and explain the observed differences, some of which are then studied; (3) Applying the results to build a full-scale interlaced lattice elastic gridshell based on the Japanese Kagome pattern.

Key words: Interlaced lattice, gridshell, timber, dynamic relaxation, numerical modeling, physical modeling, form finding, Kagome.

1. Introduction

Between 2020 and 2021 we carried out studies which enabled us to produce the ELASTICA tool [2], an ergonomic and open-source algorithm for the design and form-finding of post-formed elastic gridshells, for the verification of their structural integrity, and for editing fabrication and assembly plans. Then, we wanted to apply these results for the design and fabrication of a post-formed elastic gridshell with interlaced members.

The numerical modeling of certain types of gridshells is very complex, due to their geometry, and

the reliability of the results is difficult to assess. This is the case, for example, of non-deformable membranes in their plane, three-dimensional patterns and interlaced members.

We therefore decided to design this structure by testing physical models. The aim is to calibrate the tests using the numerical results of a "classic" gridshell, then to access the out-of-plane inertia of the interlaced gridshell and finally to extrapolate the results to scale 1. During the calibration phase, we were able to observe, analyze and study the various biases of the numerical and physical models, trying to explain why the results of the two types of models could diverge. We have deduced from this a set of recommendations and precautions to be applied to all types of elastic gridshell projects.

Corresponding author: LEYRAL Marc, Engineer Architect, Lecturer at École Nationale Supérieure d'Architecture de Paris-la Villette, research fields: post-formed elastic gridshells, braided shells, complex structures. E-mail: marc.leyral@paris-lavillette.archi.fr.

Parts of the chapters may have been reproduced with permission from: Marc Leyral, Sylvain Ebode, Pierre Guerold, Clément Berthou; *Elastica* project: dynamic relaxation for post-formed elastic gridshells, In *Inspiring the Next Generation-Proceedings of the International Conference on Spatial Structures 2020/21 (IASS2020/21-Surrey)*, edited by: Alireza Behnejad, Gerard Parke and Omidali Samavati, published by University of Surrey, Guildford, UK, in August 2021 [2]. This paper is in continuation of this work.

2. Elastic Gridshells

2.1 Definition and Origins

In architecture, a shell is a continuous thin structure with a curved surface. Its rigidity is related to its curvature (shape resistance). Thus, a gridshell is a structural lattice of bars forming a curved surface (Fig. 1).

Labbé [3] classifies gridshells into two main groups:

- “(...) those with pre-calculated members, both in their curvature and in their geometrical resolution but also in their ‘inactive-bending’ fixings,
- and those known as “active-bending” which start from an initially flat grid, which connections are not fixed until after their assembling, once the structure is established in its architectural form”.

The first category works in compression and is not the subject of this study. The elements in the second

one, called elastic gridshells, are working in flexion and compression and have two main characteristics:

- They are in active bending; the shape is given by the bending of straight elements maintained fixed. This condition is necessary to qualify a gridshell as elastic.
- They are post-formed, which means that the grid is assembled flat, not braced. The thin and hinged elements form a deformable unit that is then flexed during the erection. This condition is not necessary to be part of elastic gridshells, however our study will be placed in this framework.

The natural shape of an elastic gridshell depends on the initial grid and the displacements imposed on its support points. Let us take the simplest of them as an example: a simple flexible rod on the ends of which one pushes laterally. Initially the rod is in compression. Very slender, its equilibrium in compression by shortening quickly gives way to an unstable equilibrium in flexion: this is buckling. This can be generalized by describing a post-formed elastic gridshell as the post-buckling shape of a flat grid subjected to imposed displacements of its supports.

Once the ends of the bars are in their final position, the bent gridshell, which is by nature very deformable, must be stabilized and rigidified by adding bracing to limit the deformation of the mesh and possibly by adding shear blocks to significantly increase its out-of-plane inertia (Fig. 2). The final grid is very rigid and can cover a large span without intermediate supports, and this with very little material.



Fig. 1 Schematic typological definition of a gridshell (WIKIARQUITECTURA/Jean-Maurice Michaud/Sofia Colabella).

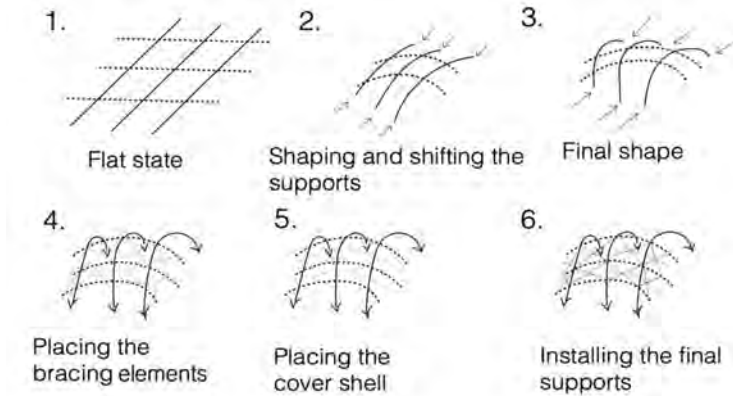


Fig. 2 Schematic typological definition of elastic gridshell (Credits: [2]).

Many people around the world have built simple shelters based on this constructive process and using only local and natural materials: wood, plant fibers, leaves, etc. (Fig. 3). The lightness of the structure is a

key advantage for their self-construction. Apart from a few exceptions like the Mongolian yurt, most vernacular gridshells are not post-formed: the stems are bent and fixed to the ground one after the other.

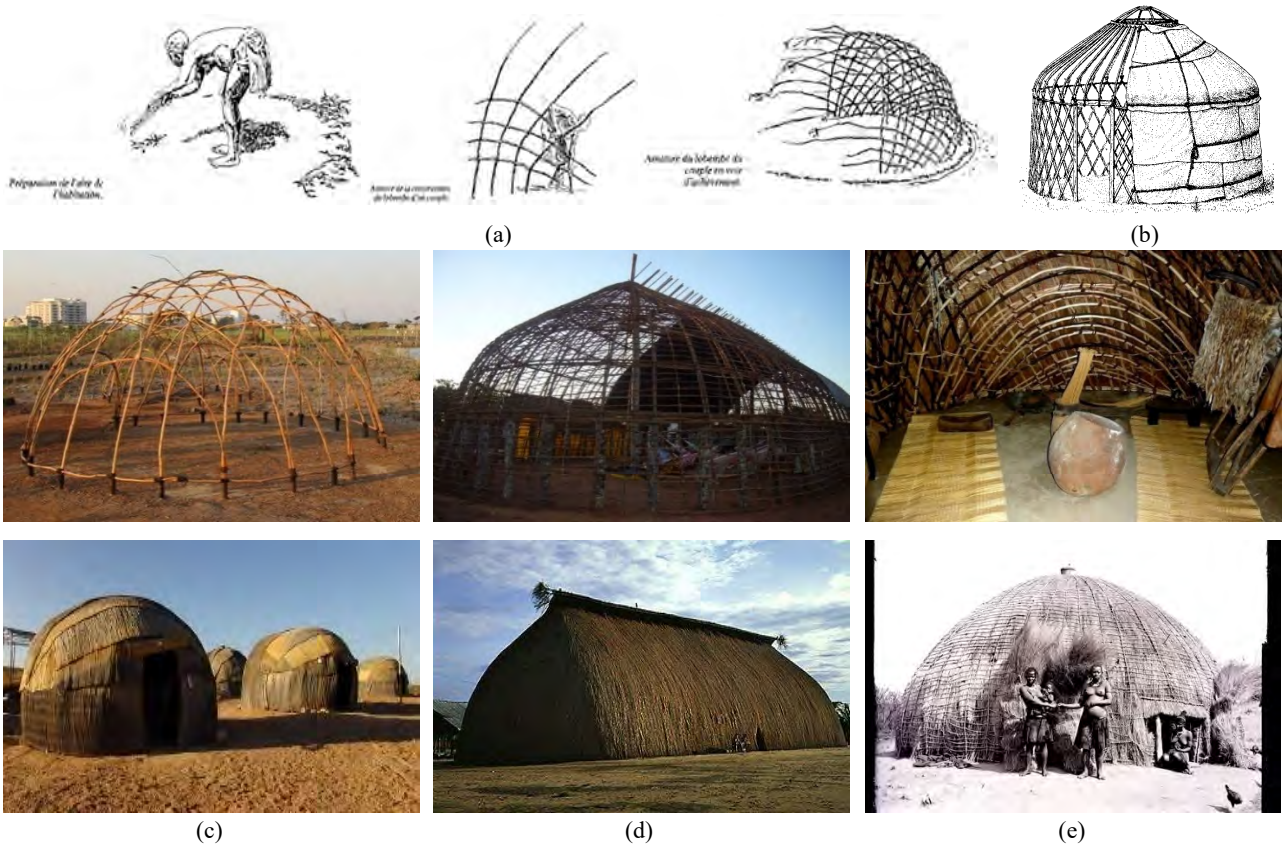


Fig. 3 Vernacular elastic gridshells: (a) Steps to build a lobembe according to Philippart de Foy [4], which is not a post-formed gridshell, (b) Post-formed gridshell: a Mongolian yurt (Smith Archive & Alamy Stock Photo), (c) Huts of the Haru Oms, Nama people (Exploring Africa/maison-monde.com), Huts of Xingu Indians (d) and Zulu tribes (e) (maison-monde.com, auroraphotos.com, John Lee, Wikimedia and africa.quora.com, Atom ref ZA 0375-N-N08935).

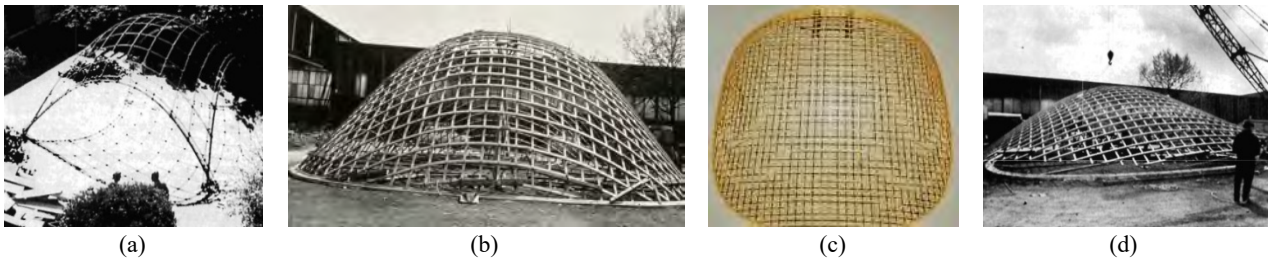


Fig. 4 (a) gridshell in Berkeley; (b) trial gridshell in Essen; (c) its model; (d) and its construction (from Ref. [1]).



Fig. 5 The Mannheim Multihalle, exterior (a) (Image by Archive Frei Otto) and interior views (b) (Archive Frei Otto and Gabriel Tang).

2.2 In Modern and Contemporary Architecture

It was not until 1962 that this typology was highlighted by the work of Frei Otto who, using a study he had been carrying out since the late 1950s on lightweight shells from suspended net models, built a first trial model of an elastic gridshell during a visit to the University of Berkeley. Later in the same year, he built a wooden trial gridshell of 198 m² at the German Building Exhibition in Deubau, Essen (Fig. 4).

Its height at the center point is 5 m. Two orthogonal layers of 60 mm × 40 mm Oregon pine elements are assembled to the floor by bolting at the knots, forming a super elliptical—or squircle—base with a mesh size of 48 cm. It was then lifted using a mobile crane and fixed to an edge beam driven into the ground.

However, the first architectural project of large scale, is undoubtedly the Multihalle in the Herzogenried Park in Mannheim (Germany), built in 1975 for the Bundesgartenschau (Fig. 5). The winning architects of

the competition, Carlfried Mutschler, Winfried Langner, and Heinz Eckebrecht, encountered difficulties in developing their idea of a free-form, airy and light structure: their proposal for large parasols suspended by helium balloons was rejected by the authorities. They then asked Frei Otto to help them, who became their engineering consultant.

The project was designed using the suspended net method, to which we will come back later, then numerically calculated and tested. The grid built on the ground is composed of two interlaced orthogonal networks, each composed by a double layer of laths 55 mm wide, forming a square mesh of 500 mm side. The knots are held by initially loose bolts to allow their rotation during erection, which was carried out using height-adjustable scaffold towers. The curved grid, still flexible at the time, is then blocked at the ends and braced to stiffen it. The western hemlock timber was shaped green and not dried because the flexibility

of the wood increases with its moisture content.

3. Design Method for Elastic Gridshells: Form Finding and Verification

Form finding can be carried out either experimentally, by means of hanging chain nets or active bending models, or numerically, for example through dynamic relaxation (RD). The work of Frei Otto, ARUP and Happold & Liddell [1], particularly on the gridshells of Essen and Mannheim, has been tested by all three methods and provides valuable data for assessing the relevance of each method.

3.1 Design with a Physical Model

3.1.1 Hanging Chain Nets Model

Hanging chain nets model is simple to realize, although it requires sliding links to make sure that all the cables are tight (Fig. 6). Its use can be surprising, since the notion of an antifunicular—and therefore pure compression—is applied to model an object in flexion and compression. To confirm its relevance, in 1973, Linkwitz digitally modeled the Mannheim model using photogrammetry. The calculations

conducted by Happold took into account the bending and led to results similar to those of the hanging chain nets.

The shape of a hanging chain (hyperbolic cosine) is determined only by its axial stiffness and a flexible rod (elastica) is determined both by its axial stiffness and by its bending stiffness. To claim that one is close to the other is therefore equivalent to saying that the bending stiffness of the flexible rod is negligible compared to its axial stiffness which is a commonly assumed hypothesis.

Let us remember that Douthe [5] studied the differences between the funicular and the elastica shape according to the attack angle α at the basis and the loading rate p (Fig. 7). He carries out this study on a simple beam, a rectangular grid and a free-form grid. He concludes that the shape of the gridshell is almost funicular if the angle of attack α is less than 65° (optimum at 57.5°), which corresponds to a pL^3/EI ratio below 65, confirming a posteriori the modelling of Mannheim by Frei Otto. Like Happold and Liddell [1], we can therefore conclude that “a funicular shape is an advantage but is not essential.”

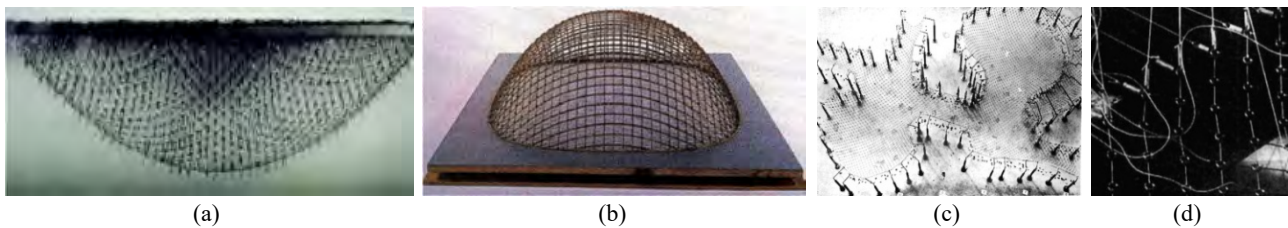


Fig. 6 Hanging chain net (a) and active-bending models (b) of the trial gridshell in Essen; (c) hanging chain net model of the Mannheim Multihalle; (d) zoom on the links (www.freiotto.com, Architekturmuseum TU München and from Ref. [1]).

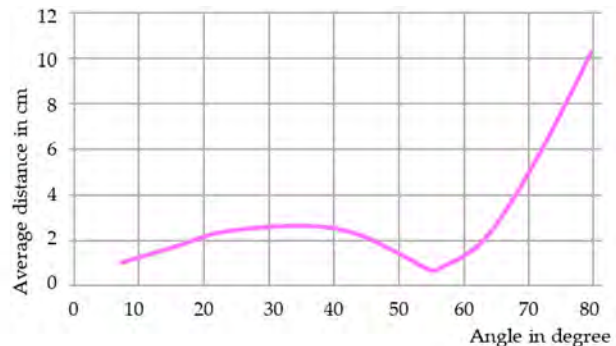
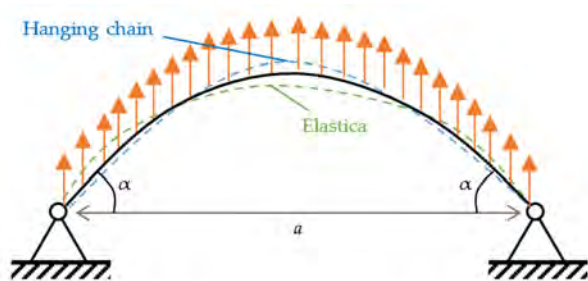


Fig. 7 (a) Diagram of the problem studied by Douthe [5]; (b) evolution of the distance to the hanging chain form with the angle α .

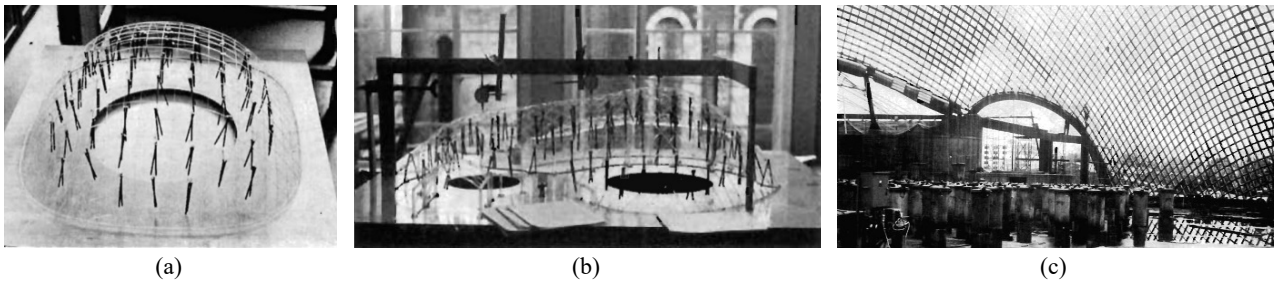


Fig. 8 Load test by adding nails to the nodes of the Essen (a) and Mannheim (b) models; (c) loading tests with water-filled garbage cans (from Ian Liddell and from Ref. [1]).

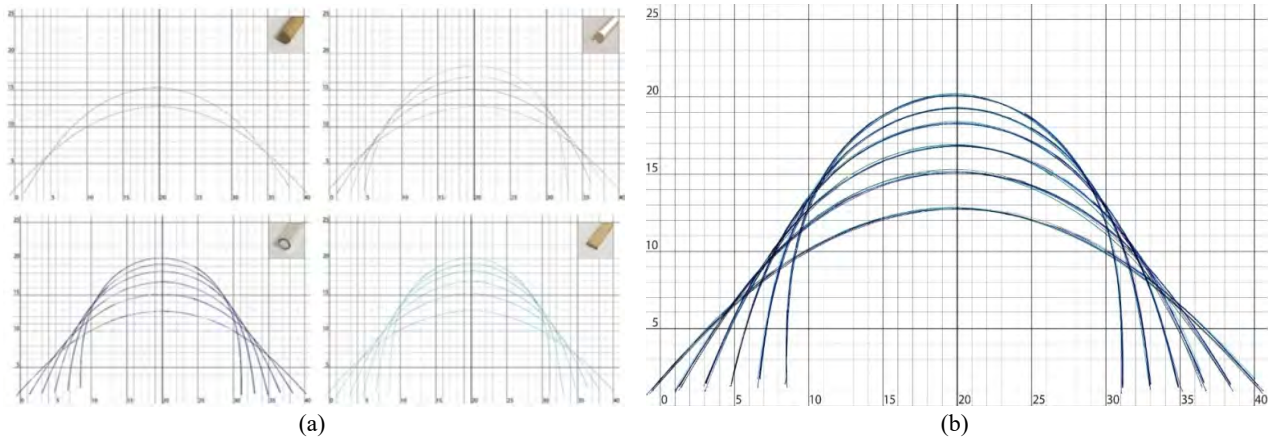


Fig. 9 Scalability tests on the section and stiffness of the material (a) and on the length of the element (b) (from Ref. [2]).

3.1.2 Active Bending Physical Model

In 1973, as Happold and Liddell [1] reminded us, “there was no previous engineering experience in this field.” To overcome this, his team first studied a simpler example by loading a PMMA (polymethyl methacrylate) model at the 1/16th scale of the trial gridshell in Essen and comparing the results with the data collected by the Warmbronn Workshop on the actual project. The tests were conducted with pinned or rigidly glued nodes and with or without bracing. The team found, and retained for the Mannheim project, that the addition of bracing on the diagonals of the lattice reduced deflection and increased the maximum nodal load causing buckling of the shell, but that the collapse was more sudden.

An active bending model of the Multihalle was then fabricated in PMMA at 1/60th scale and tested in the same way. The buckling collapse load of the model was measured at 2.8 kg/m² without bracing and at 12.5 kg/m² with bracing (Fig. 8). Happold and Liddell demonstrate that an extrapolation of the critical load is possible from a model to a real project by multiplying

it by the ratio of EI_{xx}/aS^3 of the project and the model (EI_{xx} is the out-of-plane bending stiffness, a the spacing of laths and S the gridshell span).

From these studies and our previous experiences on the essential question of the extrapolation of the results from the model to the real project, we first concluded that:

- The shape of a funicular and the shape of an elastic gridshell can be transposed from the model to the real project, regardless of the stiffness, the section and length of the material used (Fig. 9).
- The buckling force is transposable but subjected to several measurement biases.
- The shear and node stiffness are difficult to transpose, and this may reduce the relevance of the results of the previous point.

3.2 Design with a Numerical Model by Dynamic Relaxation

To overcome the inaccuracies of a form finding with a physical model, a numerical method is

generally necessary. We developed our own algorithm on Rhino + Grasshopper. Called ELASTICA, it is a complete, generic, open-source and ergonomic tool, usable by all, for form-finding, dimensioning, and optimization of elastic gridshells using dynamic relaxation. The theory of dynamic relaxation and the elaboration of ELASTICA algorithm are given in Appendix A. We will focus in the following on the analysis of the results obtained by physical and numerical models on a gridshell project.

4. Numerical and Experimental Design

4.1 Presentation of the Studied Gridshells

The project takes place on the belvedere of the

Butte du Chapeau Rouge Park, in the 19th arrondissement of Paris. Built from 1938 by Léon Azéma, then by his son Jean, the park is bordered by “Habitations à Bon Marché” (French housing at low rent during the first half of the 20th century) built with concrete and red bricks and offers a breathtaking view of the Saint-Denis plain below.

It is in this context that we built in 2020 a first post-formed elastic gridshell of “classic” design, Elastica. In July 2022, we plan to complete the initial project by building a second post-formed elastic gridshell, Kagome, which will be different because it will be made by interlaced lattices in three directions (Figs. 10 and 11).

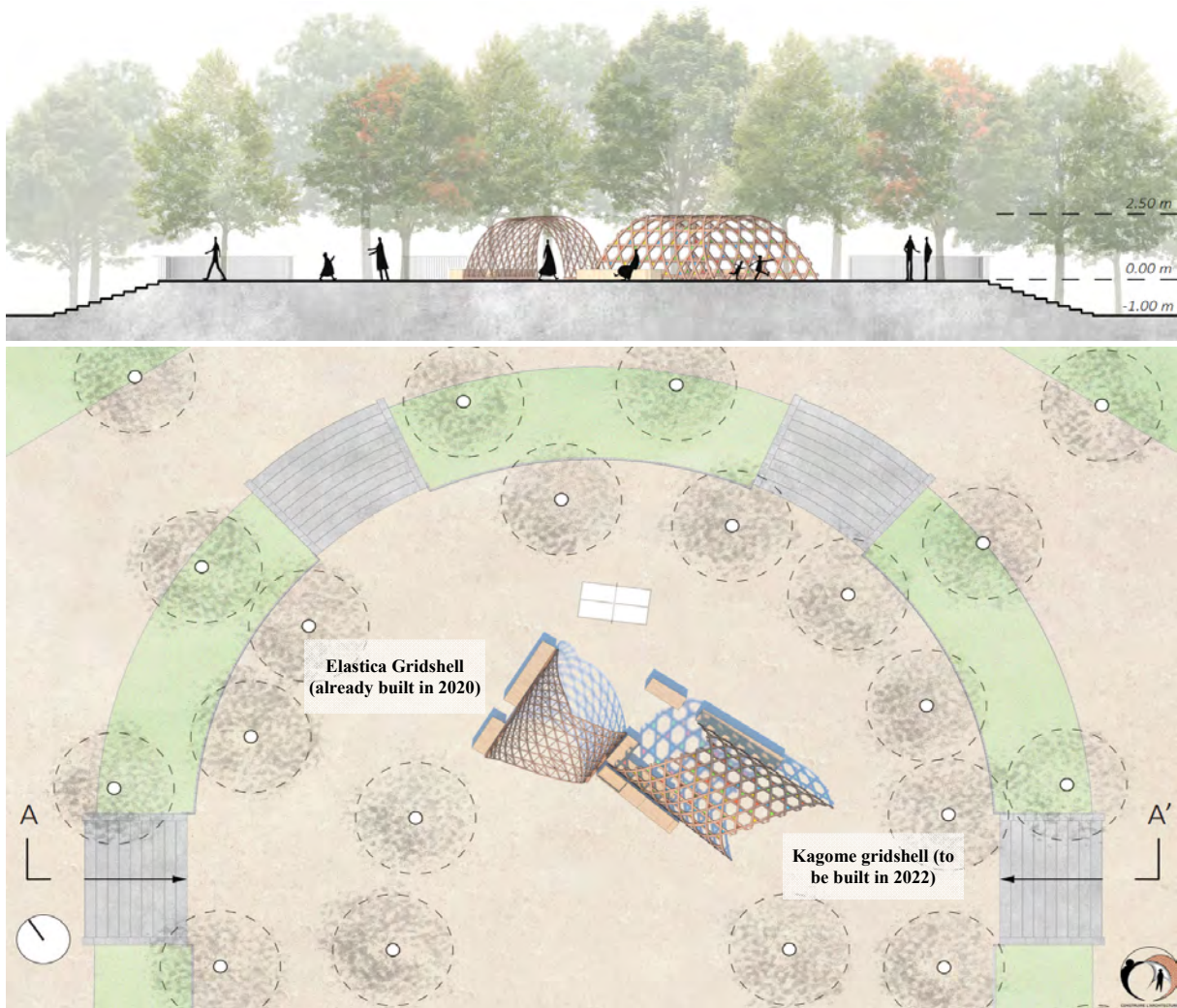


Fig. 10 Elevation and masterplan of the studied gridshells.

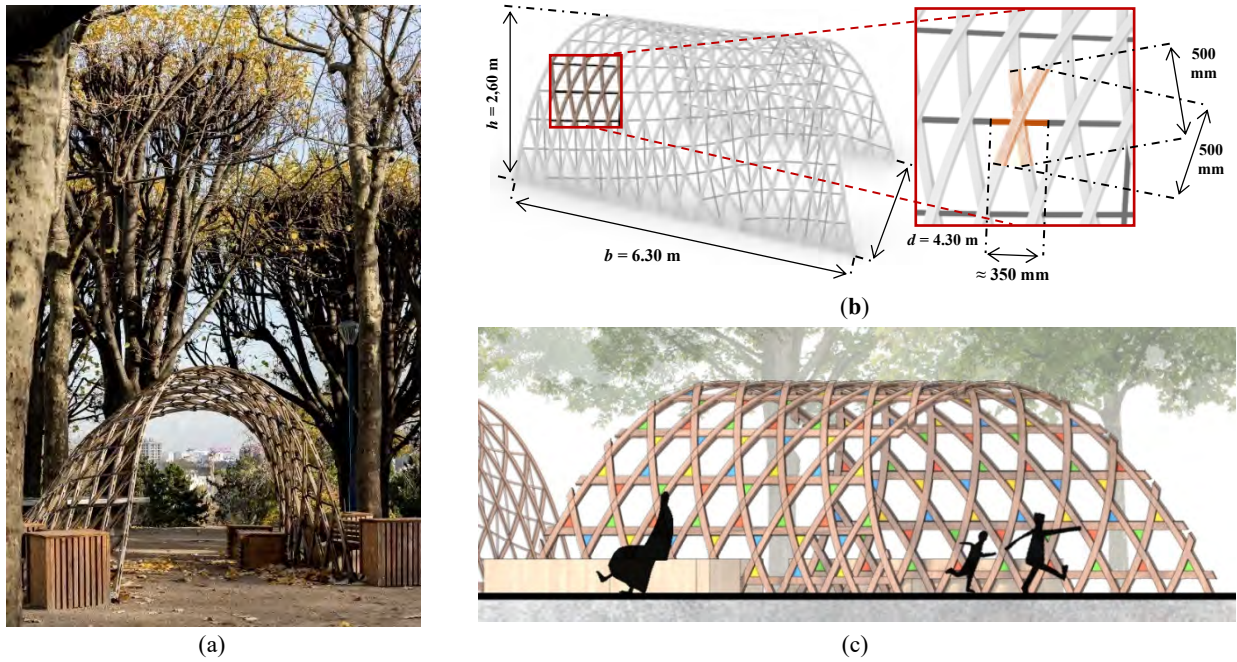


Fig. 11 (a) Gridshell Elastica, 2020 (Credits: Salem Mostefaoui), main dimensions (b), and 3D du gridshell Kagome (c).

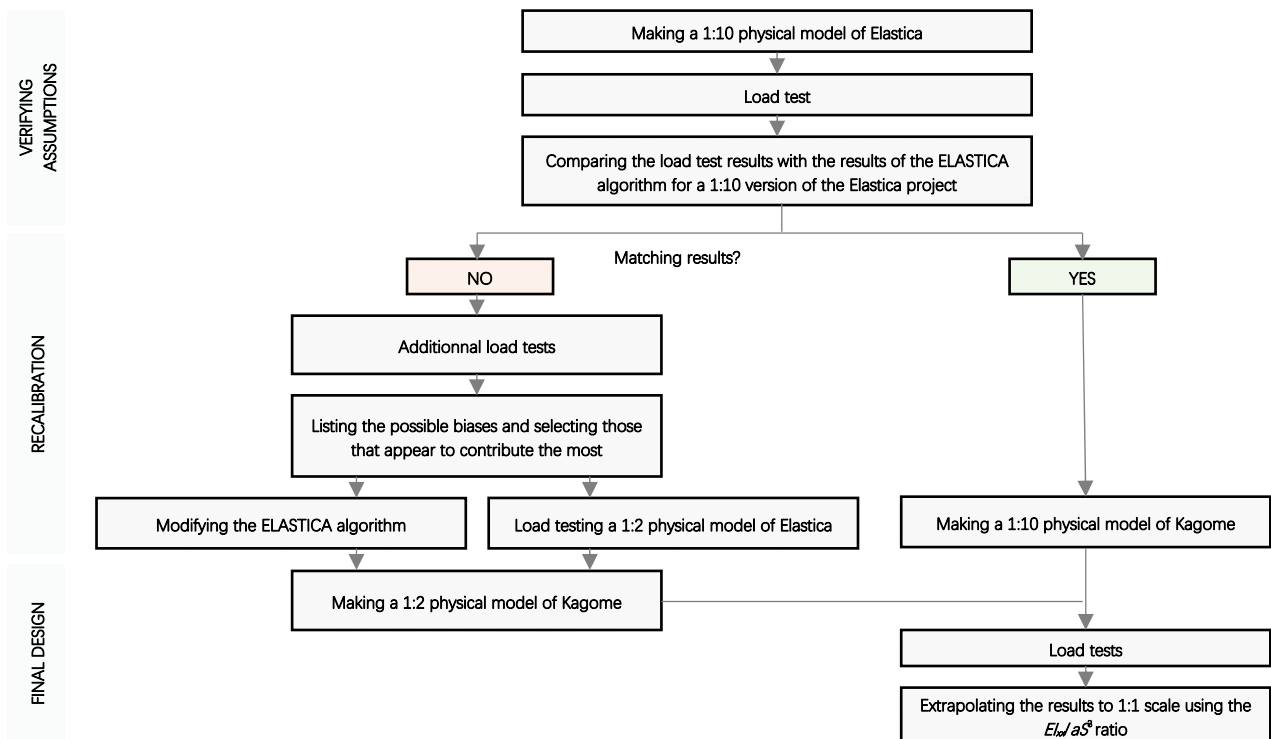


Fig. 12 Methodology developed for the design of the Kagome gridshell.

4.2 Issue and Methodology

Issue: Kagome is not directly accessible to numerical calculation with the ELASTICA algorithm (Fig. 12) because:

(1) It is already braced when built flat (because of the three-direction pattern). There is therefore no movement possible between the lattices in plan, and this is true from the erection phase to the loading phase.

(2) The evaluation of the out-of-plane inertia is complicated by the lathing in three directions and the method of assembly by interlacing the lattices.

4.3 Consolidation Phase

4.3.1 Numerical Calculation of the Elastica Project Using ELASTICA Algorithm

Load assumptions (nodal loads):

- Service Limit State: for deflections’ calculation.

However, as the pavilion is temporary, no limit is imposed on this serviceability criterion and creep in timber is neglected.

$$1.00 G = 1.26 \text{ kg}$$

$$1.00 G + 1.00 W + 0.60 S = 5.97 \text{ kg}$$

- Ultimate Limit State (ULS): a safety criterion: loads combinations for stress and surface’s buckling verifications.

$$1.35 G = 1.70 \text{ kg}$$

$$1.35 G + 1.50 W + 1.05 S = 9.09 \text{ kg}$$

A safety factor on the results of the calculations considering various uncertainties (variations in modulus of elasticity E —due to natural inhomogeneity, moisture and creep—accuracy of shape of shell, variations in loading, accuracy of computer model and assumptions, nature and significance of buckling collapse, consequences of failure) of 3.46 has been

applied on the ULS.

Buckling limit load of the surface: predominant ruin mode for gridshells. To determine the critical buckling load, we proceeded by dichotomy on loads in the ELASTICA algorithm. We tested all the main design parameters: lathing type (single layer or double layer), the use or not of bracing, the use or not of shear blocks (cf. Table 1 and Fig. 14). To interpret these results, we compared them with those obtained by model and numerical modelling by Happold and Liddell [1] for the Mannheim Multihall (Fig. 13 and Table 2).

According to Happold and Liddell, all other things being equal, the use of bracing on double lathing increases the critical load by a factor of between 1.60 and 4.44. Furthermore, we can predict that the addition of shear blocks will increase the critical buckling load by a factor of about 13, determined by the ratio of inertias with $(26bh^3/12)$ and without $(2bh^3/12)$ these blocks. As for the results of our modeling of the Elastica project, we can conclude that, all other things being equal, buckling resistance is increasing:

- By a factor of 2.00 to 2.02 by designing a double layer grid.
- By a factor of 1.81 to 1.83 adding bracing.
- By a factor of 11.09 to 12.29 adding shear blocks.

Table 1 Parameters of the ELASTICA algorithm for the Elastica project.

Input data	Symbol	Value	Unit	Mechanical parameters	Symbol	Formula	Unit	
Lath width	b	0.045	m	Surface	Simple layer grid	bh	m^2	
Lath height	h	0.012	m		Double layer grid	$2bh$		
Initial mesh length	L_0	0.5	m	Nodal mass		m	$V\rho+ma$	kg
Mass of the connecting element	m_a	0.4	kg	Simple layer		$bh^3/12$		
Timber density	ρ	500	kg/m ³	Inertia	Double layer without shear blocks	I	$2bh^3/12$	m^4
Timber modulus of elasticity E		11,500	MPa		Double layer with shear blocks		$26bh^3/12$	
				Axial stiffness		R_a	EA/L_0	MN/m
				Bending stiffness		R_f	$2EI/L_0^3$	MN/m

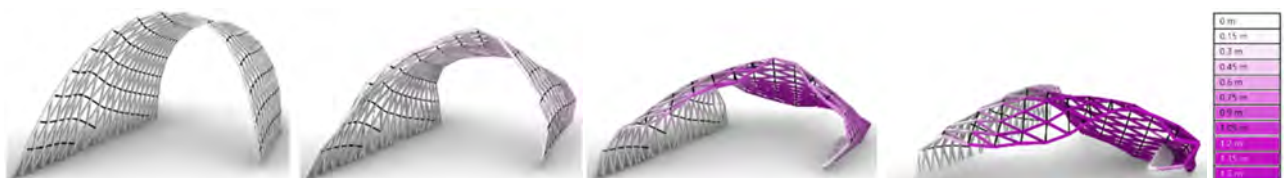


Fig. 13 Kinematics of gridshell’s global buckling when nodal loads exceed critical load (from Ref. [2]).

Table 2 Critical buckling loads for Elastica and Mannheim gridshells.

Layer	Bracing	Shear blocks	Critical nodal load Elastica (kg at each node) ^{***}	Critical nodal load Mannheim (kg/m ²) ^{***}
Simple	no	n/a	1.05	3.8 ^{**}
	yes	n/a	1.90	Non-evaluated
Double	no	no	2.10	63 ^{***} /100 ^{**}
	no	yes	25.80	-
	yes	no	3.85	100 [*] /160 ^{**} /280 ^{***}
	yes	yes	42.70	-

^{*} Results of the numerical model.
^{**} Extrapolated predictions based on the Essen model.
^{***} Results extrapolated on the basis of the Multihall model.

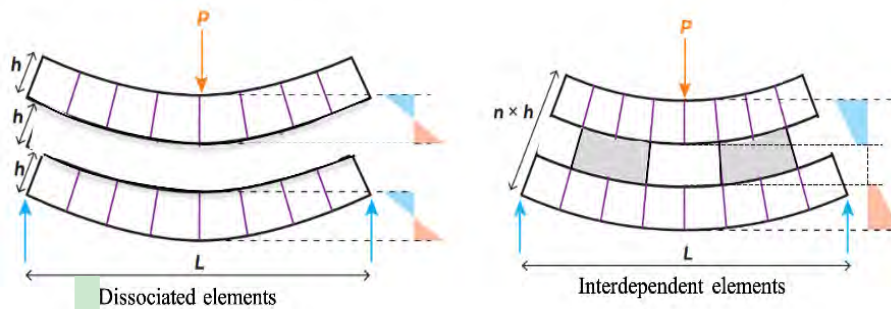


Fig. 14 Principle of increasing inertia by connecting the layers with shear blocks (from Ref. [2]).

These results correlate with our theoretical predictions and with Happold and Liddell’s analyses. We also wished to compare them with the formula proposed by Douthe [5] who believes that “in order to obtain an expression of the critical pressure p_{cr} that will cause the shell to collapse, it is assumed that this load is close to that which causes the instability of an equivalent cylindrical shell subjected to hydrostatic loading, i.e. of the type: $p_{cr} = 3EI/R^3$ ” (I is here the inertia per unit of length). The proximity to the results on the three designs tested (cf. Table 3) – the radius of curvature, 2.4 m, is measured at the median curvilinear position – shows a correlation between the buckling of a gridshell and that of a cylindrical shell, giving an a priori validation of the hypothesis.

We concluded from this study that Elastica should be a double-layered gridshell with bracing and shear blocks (Fig. 15).

4.3.2 Loading Tests on a 1:10 Physical Model of Elastica

Following the studies described so far, the Elastica gridshell was built in September 2020. The initial

objective of our research in 2022 was to theorize the extrapolation of these results for the design of gridshells with different lathing such as the Kagome gridshell.

However, during the development of the ELASTICA tool, the Covid-19 prevented physical meetings of the team and studies on real models could not be carried out. In 2022, we therefore decided to check the validity of our digital tools upstream by comparing them to load tests on 1:10 scale models (Fig. 16).

Let us recall that during the studies of the Mannheim Multihalle by Happold and Liddell [1], the buckling collapse load of a physical model was measured at 2.8 kg/m² without bracing and at 12.5 kg/m² with it. An extrapolation of the critical load being possible from a model to a real project by multiplying it by the ratio of the EI_{xx}/aS^3 of the project and the model (I_{xx} being the out-of-plane inertia, a the spacing of the lattices and S the span of the gridshell), the structure’s collapse load is thus assessed at 63 kg/m² for double lathing without bracing and at 280 kg/m²

Table 3 Critical buckling loads by the ELASTICA algorithm and the formula of cylindrical shells.

Layer	Bracing	Shear blocks	Critical nodal load by modelling (kg)	Critical nodal load calculated with $p_{cr} = 3EI/R^3$ (kg)
Simple	no	n/a	1.05	1.02
Double	no	no	2.10	2.05
	no	yes	25.80	26.71

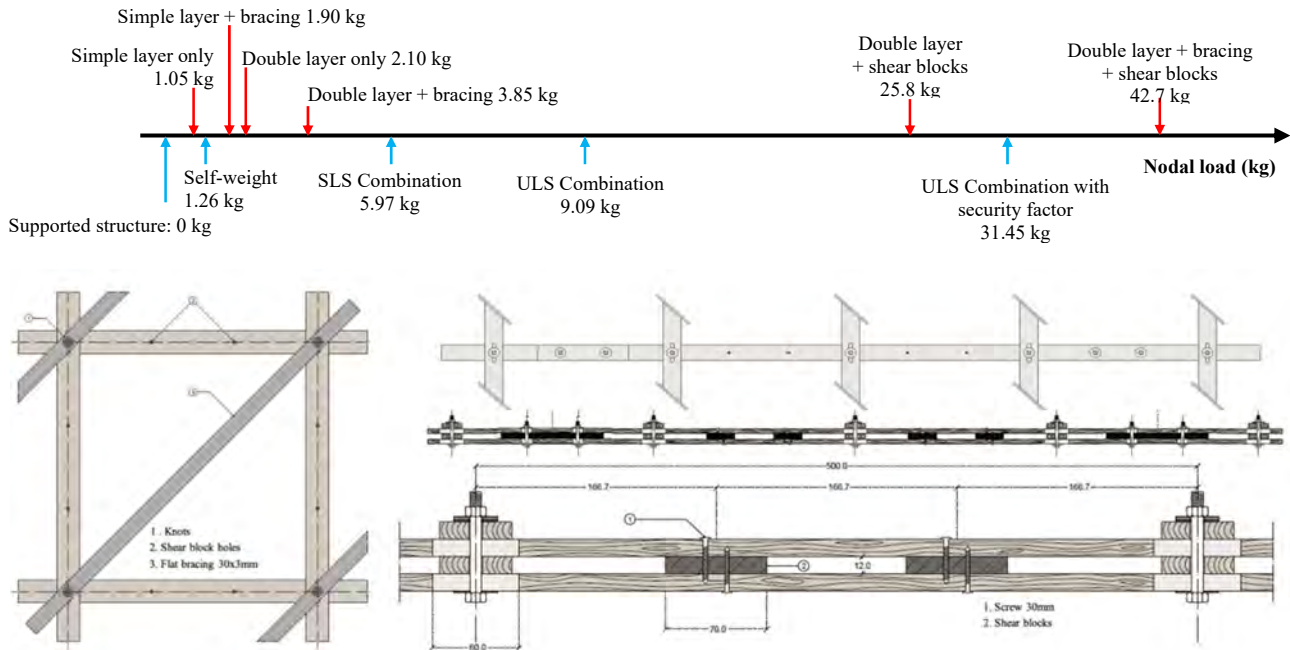


Fig. 15 Synthesis of the project loads and critical buckling loads according to the different possible designs, and details of the Elastica gridshell: our study shows that the expected loads on the Elastica gridshell require a double lath design with bracing and shear blocks.

Table 4 Comparison between the numerical and experimental results on the post-formed elastic gridshell Elastica in its version with simple lathing and without bracing.

G01: Elastic gridshell with simple lathing and without bracing						
Parameters	Scale model 1:10			Real project 1:1		
	Load test on the physical model	Numerical simulation (RD)	Comparison to cylinder shells	Extrapolation by upscaling 1:10 result	Comparison to cylinder shells	Numerical simulation (RD)
Radius of curvature at the center R						
Lattice section $b \times h$						
Number of nodes by m^2						
Gridshell span S /distance between lattices a						
Timber elastic modulus						
Buckling critical load	0.027 kg (0)	0.011 kg (0)	0.011 kg (1)	2.80 kg (2)	0.92 (1)	1.05 kg (0)
Lattice inertia I_{xx}	2.358 mm^4 (1)	0.83 mm^4		21,468 mm^4		7,200 mm^4
Inertia by length unit I	0.047 mm^4/mm (1)	0.017 mm^4/mm		42.9 mm^4/mm		14.4 mm^4/mm

(0) By direct measure (physical model) or by dichotomy (using ELASTICA algorithm).

(1) Buckling critical load of a cylindric shell under hydrostatic load: $p_{cr} = 3EI/R^3$.

(2) Extrapolated using the EI_{xx}/aS^3 between the model and the project.

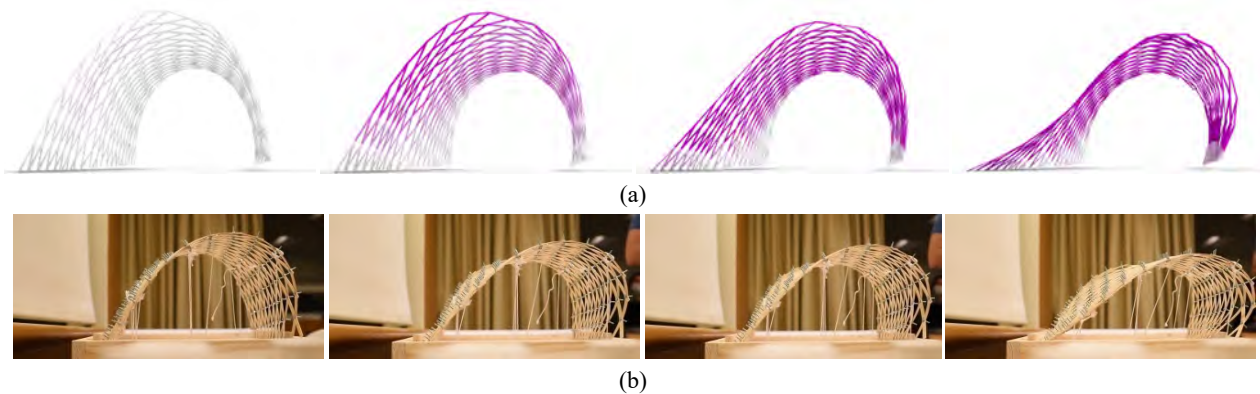


Fig. 16 Buckling kinematics predicted by ELASTICA (a) and on a 1:10 model of the Elastica project (b) at approximately 35%, 80%, 90% and 99% of their respective critical buckling load.

with it. However, numerical calculations predicted are 100 kg/m^2 . The study attributes the difference, a factor of 2.8, to the non-variability of scale of the stiffness in shear or to a greater stiffness of the nodes of the scale model.

4.3.3 Conclusion of the Consolidation Phase

The results of the “calibration” test show that the critical buckling load of the scale model is 2.48 to 2.53 times greater than anticipated by the calculation via the dynamic relaxation simulation (Table 4). This non-negligible ratio is quite close to that observed by Happold and Liddell on Mannheim (2.80).

To try to understand it, let us come back to the reflections of Happold and Liddell [1] on the extrapolation of the results on a scale model. The authors identified several properties of the structure “which define and control its behaviour. [They] are listed as follows:

S = Span. If the model is geometrically scaled then its size can be represented by a typical dimension, say the span

EI_{xx}/a = The out of plane bending stiffness of the surface a per unit length (a = spacing of laths)

EI_{yy}/a^3 = [The in-plane bending stiffness] is proportional to the contribution of the timber members to diagonal stiffness, if the joints between timber members are rigid

EA/a is the axial stiffness along the timber members per unit length

$E'A'/ka$ = is proportional to the contribution of the

ties to the diagonal stiffness ([...] ka being the tie spacing)”. List to which is added a contribution related to the slip per unit force of each node.

We then undertake the following reasoning in order to determine the parameters that seem to us to be the most significant in their contribution to the differences observed:

As “the deformation of the grid shell is mainly due to out-of-plane bending and diagonal distortions of the grid squares [and] if the diagonal stiffness is much less than the axial stiffness” [1], we will consider as negligible the contribution of the axial stiffness of the lattices with respect to the out-of-plane bending stiffness.

As the tested gridshell is designed without bracing, the contribution of the bracing elements’ axial stiffness $E'A'$ has no place in the reflection.

In agreement with Happold and Liddell, we will say that if the bracings have a very high axial stiffness, the contribution of the stiffness in plan is negligible. However, the tested gridshell had no bracing.

We therefore identify at this stage the two parameters on which we will focus our evaluation:

(1) Semi-rigid nodes. The contribution of the nodes which are modeled in dynamic relaxation as perfectly articulated in the plane whereas they in fact have a certain stiffness due to the tightening of the assembly and the friction induced by the curvature of the lattices.

To evaluate this parameter, we will:

- Carry out loading tests on braced models, because the blocking of the deformation of the mesh induced by the axial stiffness of the braces, if it is large enough, should make the numerical and physical results converge.

- Modify the ELASTICA algorithm to take into account a spring torque in rotational friction at each node, compare the results obtained with loading tests on models at 1:10 and 1:2 scales. The contribution of friction, which tends to fictitiously increase the extrapolated critical load, should decrease with the increase of the scale of the physical model.

(2) In-plane bending stiffness. Moreover, considering this nodes' rotational stiffness implies a possible mobilization of the in-plane bending stiffness of the lattices, since it allows the deformation by bending of the elements inside the local plane of the surface, which is only possible if the nodes are semi-rigid (Fig. 17). To analyze this contribution, we will modify ELASTICA to take into account a biaxial bending of the timber elements.

In addition, each model, numerical or physical, includes a set of biases, the nature of which should be listed and, if possible, the deviations they may cause in the result should be assessed. These are mainly geometric imperfections and model loading imperfections, which are all the more important as the model is reduced. We will devote part of our analysis to them.



Fig. 17 (a) Hinged nodes; (b) semi-rigid nodes: bending in the plane of the lattices is only possible if the nodes are semi-rigid.

4.4 Recalibration Phase

4.4.1 Loading Tests on a 1:10 Scale Model with Loose Connections

In order to reduce as much as possible the contribution of the stiffness of the nodes and—possibly—of the bending in the plane of the lattices, we carried out a new test on the 1:10 model, loosening the nodes as much as possible. The results of this test give a critical buckling load of the model at 0.0177 kg per node, i.e. a deviation of 1.61 to 1.65 with the numerical predictions. A preliminary result motivates us to study more precisely the contribution of the rotational stiffness of the connections and that of the in-plane bending stiffness of the lattices in the evaluation of the critical load of the tests.

4.4.2 Loading Tests on a 1:10 Scale Model with Bracings

In order to go further in this reflection, we carried out a loading test on a 1:10 braced model (Fig. 18). If our assumption is correct, and since the axial stiffness per unit length of the braces $E'A'/ka$ is large enough, the possible contributions of the rotational stiffness of the nodes and the out-of-plane bending stiffness of the chords should be negligible.

The results of this experiment show a difference of only 1.5% between the physical model (0.0182 kg per node) and the numerical model (0.0185 kg per node).

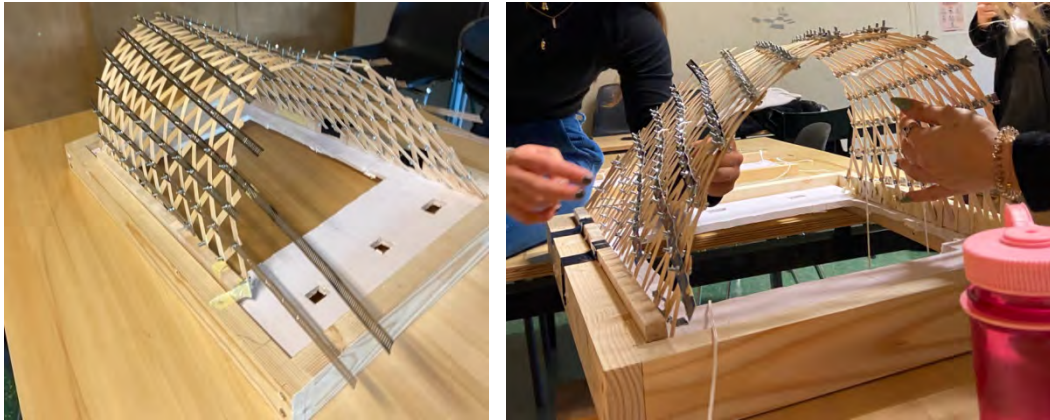


Fig. 18 Loading tests on a 1:10 scale model with bracings (single layer).

4.4.3 Preliminary Outcomes

These results tend to confirm our hypotheses on the contribution on the critical load of buckling of the rotational stiffness of the nodes and—possibly—of the in-plane bending stiffness of the timber lattices in the case of an unbraced gridshell. However, these results should be considered with great caution at this stage because:

- The number of trials is very low.
- At this scale, the biases linked to geometric imperfections and to the loading protocol—we only loaded 1 node out of approximately 15 on the model—are probably significant and their contributions to the results are still poorly controlled.
- We could not scale the bolts and therefore the washers. They are proportionally larger and mechanically increase the friction at the nodes and therefore their stiffness. It is a fact that the difference in the physical tests between the model with the loose nodes (0.0177 kg per node) and the braced gridshell model (0.0182 kg per node) suggests that once the shell has been shaped, the friction between the bolts of the nodes and the lattices plays a non-negligible role in blocking by friction, especially as the scale of the model is reduced and the scale of the bolts is proportionally larger compared to that lattices. However, this bias does not contradict—on the contrary—our previous interpretations.
- These conclusions would imply that the consistency

between the critical buckling load of a gridshell (braced or not) and that of a cylinder shell subjected to hydrostatic pressure is valid only on a sufficiently large scale. We note that a cylindrical shell has no possible movements in the plane of its surface.

- We did not test a simple and symmetrical cylindrical vault but the project of architecture students from ENSA-Paris la Villette, which presents a strong asymmetry. Subsequent tests showed that this asymmetry reduced the critical buckling load by 33% according to the physical tests on a 1:10 scale model and by 46% according to the extrapolated numerical model (Fig. 19). We also noticed that this asymmetry very substantially increased the sensitivity of the loading imperfection (depending on the position of the loads, the result could vary by 56%).

We conclude that additional tests on a 1:2 scale model are necessary in order to assess the impact of imperfections in the result. Indeed, on a larger scale, the loading and geometry imperfections and also the nodes friction will be reduced. A modification of the ELASTICA algorithm taking into account the rotational stiffness of the nodes and the in-plane bending stiffness of the lattices will also make it possible to compare the new physical results to numerical ones.

4.4.4 Methodology for the Analysis of the Contribution of Rotational Stiffness of Nodes

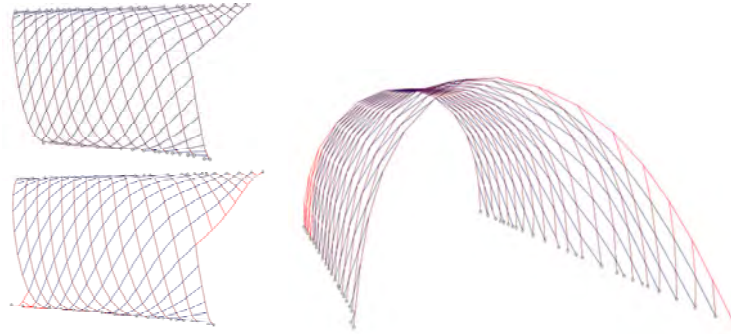


Fig. 19 Effect of gridshell symmetry: adding only the red parts increased the critical buckling load of Elastica by 86% according to the numerical simulation. A similar modification on Kagome led to an increase of 50% according to a loading test on a 1:10 physical model.

Taking into account the rotational stiffness of the nodes: it is modeled at each node by a spring force F_f proportional to the rotation angle θ between the two directions of the lattices (Fig. 20):

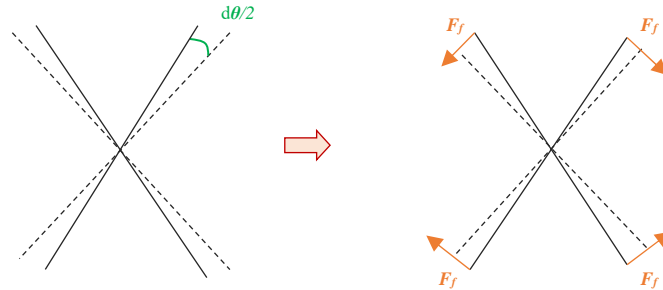


Fig. 20 Spring force due to the friction opposing the relative rotation of the lattices.

It combines the contribution of:

(1) a tightening force N_{ser} equal to 90% of the elastic limit of the wood perpendicular to the fibers $\sigma_{y,w,90}$ multiplied by the washer area A_r :

$$N_{ser} = 0,9 * \sigma_{y,w,90} * A_r \tag{1}$$

(2) a force N_{con} linked to the contact between the lattices of the 2 opposite directions when the curvature of one exceeds a limit defined by an average slack (Fig. 21):

$$N_{con} = (F_{i-1,i} + F_{i,i+1}) * \cos(\alpha_i) \approx \frac{4EI \sin(\alpha_i) \cos(\alpha_i)}{L_0^2} \tag{2}$$

$$N_{ser} = (F_{i-1,i} + F_{i,i+1}) * \cos(\alpha_i) \approx \frac{4EI \sin(\alpha_i) \cos(\alpha_i)}{L_0^2}$$

$$F_f = \frac{M_r}{L_0} = \frac{\alpha_{fr} * (N_{ser} + N_{con}) * b}{2 * L_0} \tag{4}$$

The bearing moment M_r equals then:

$$M_r = \alpha_{fr} * (N_{ser} + N_{con}) * \frac{b}{2} \tag{3}$$

where α_{fr} is the static friction coefficient of wood-on-wood.

Hence the fictitious force F_f :

We carry out numerical tests with and without tightening of the assemblies. The contact force N_{con} is applied only if the curvature is sufficient to create the contact. With one-millimeter tolerance in assemblage, contact appears in about one-third to one-half of the gridshell nodes, according to our testing. The results are presented in Tables 7-9.

$$F_{i-1,i} = \frac{2EI \sin(\alpha_i)}{L_{i-1,i} * L_{i-1,i+1}}$$

$$F_{i,i+1} = \frac{2EI \sin(\alpha_i)}{L_{i,i+1} * L_{i-1,i+1}}$$

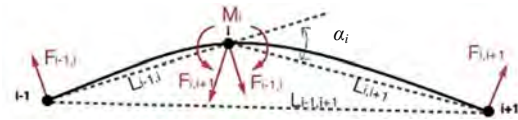


Fig. 21 Forces due to bending (see Appendix A).

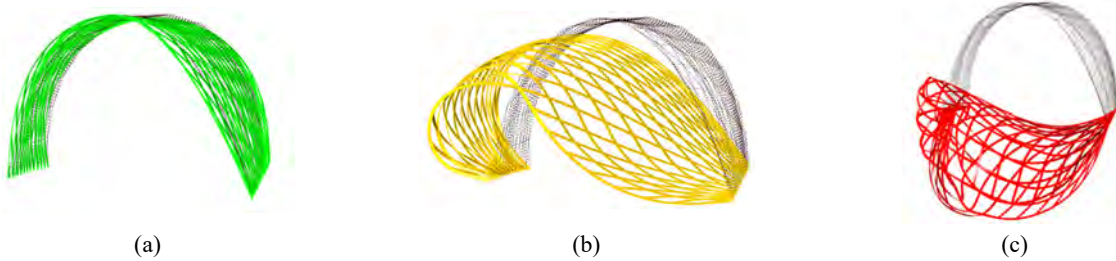


Fig. 22 (a) “Arch” gridshell; (b) “critical” gridshell; (c) “collapsed” gridshell.

Table 5 Model data for the 1:2 scale model of Elastica (single layer version, no bracings).

Parameters	Model 1:2	Project
Radius of curvature at the center R	1.20 m	2.40 m
Lattice section $b \times h$	24 mm \times 7 mm	50 mm \times 12 mm
Number of nodes by m^2	16	4
Gridshell span S /Distance between lattices a	1.78 m/250 mm	3.56 m/500 mm
Timber elastic modulus	11,500 MPa	11,500 MPa

Table 6 Comparison and calibration of the physical tests for the 1:2 scale model of Elastica.

Models	Buckling start (RD)	Rupture (physical)	End of buckling (RD)
-	Load: 57.15 kg	Load: 65.00 kg	Load 74.14 kg

During these more precise tests, we realized that there were in fact three distinct states on our model which prompted us to define more stages of global buckling load on the structure instead of one. In order to correctly characterize the observed results, we define them in Fig. 22.

Finally, a half-scale model was produced for the purpose of loading tests (Table 5). During this experiment, only the 73 most critical to buckling nodes were loaded (out of 203 nodes in total). This induces a loading bias that must therefore be corrected using a numerical test where the own weight of the

gridshell is distributed over all the nodes, but the additional load is applied over the 73 selected nodes only (Table 6).

It should also be noted that the condition of the collapse occurred in the model at an earlier load compared to the dynamic relaxation modelisation. This is due to the fact that in dynamic relaxation, the bars are considered to be infinitely resistant, allowing a complete overturning of the gridshell. In reality, this geometric deformation generates a localized drop in the radii of curvature and therefore an increase in the stress which will exceed the breaking stress limit of the wood (Fig.24). This observation invites to introduce a safety coefficient on the result of the dynamic relaxation that our present study places around 1.15.

4.4.5 Methodology for the Analysis of the Contribution of the In-Plane Bending Stiffness

As explained in Appendix A, on a given lattice, for a series of 3 consecutive points A, B, C, the forces due to the bending moment belong to the plane (ABC). These forces are then proportional to the sine of angle α between \overrightarrow{AB} and \overrightarrow{BC} and to the inertia of the section. Until now, ELASTICA tool has considered a bending of the laths in the “weak” direction ($I_{xx} = b * h^3/12$), thus as if the lath’s bending was entirely in the plane perpendicular to the gridshell’s surface plane. This assumes that the generative curves of the “arch” are single curvature, which is not the case. In reality, the laths are in bi-axial bending: in the weak direction as previously described (out-of-plane bending) and in the shell surface (in-plane bending). The latter therefore involves the strong sense of inertia ($I_{yy} = h * b^3/12$).

To take this into account, we construct two planes (Fig. 23): a plane T_B which is the tangent to the shell at point B (a smooth surface is defined by interpolation of the nodes of the gridshell at each time step of the dynamic relaxation), and a plane N_B which contains the normal to the surface at point B and line

(AC). Taking in-plane stiffness into account means that the planes (ABC) and N_B are not identical. We project point B on plane N_B (obtaining B’) and points A and C on plane T_B (obtaining A’’ and C’’), then we calculate the forces due to bending in each plane.

4.4.6 Results of Physical and Numerical Loading Tests

The compared results of the tests relating to the rotational stiffness of the nodes and in-plane bending stiffness on physical models and on numerical models are given in Tables 7-9.

It is noted that the difference between scale model and numerical simulation is greatly reduced when the rotational stiffness of the nodes is taken into account in the calculation: it is for example of the order of 4% on the tests on the 1:10 model. However, taking these parameters into account requires a “guesswork” evaluation of the actual tolerance in the connections and of the tightening force of the nuts. We also observe that the contribution of in-plane bending stiffness has a very little effect on the results.

The second observation is that the contribution of the rotational stiffness of the nodes decreases with the scale of the model, thus—on this precise parameter—we could conclude that the numerical simulation should give results close to reality at scale 1 and that this is especially true if the gridshell is braced.

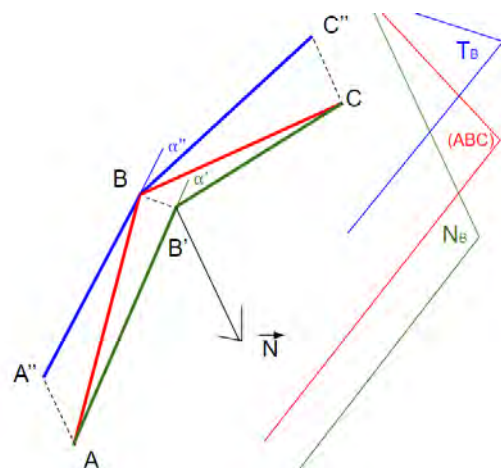


Fig. 23 Definition of the planes used to evaluate bi-axial bending.

Table 7 Impact of rotational stiffness of nodes on numerical and physical tests at a 1:10 scale.

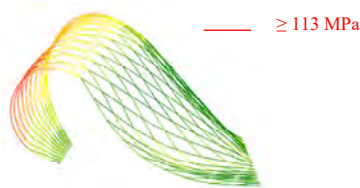
Type of test	0.010 kg	0.011 kg	0.013 kg	0.015 kg	0.016 kg	0.017 kg	0.018 kg	0.021 kg	0.026 kg	0.027 kg
Dynamic relaxation with articulated nodes										
Dynamic relaxation with friction and loose connections										
Physical test, loose connections										
Dynamic relaxation with friction and tight connections										
Dynamic relaxation with friction and tight connections considering in-plane stiffness										
Physical test, tight connections										

Table 8 Impact of rotational stiffness of nodes on numerical and physical tests at a 1:2 scale.

Type of test	0.40 kg	0.45 kg	0.50 kg	0.55 kg	0.60 kg	0.65 kg
Dynamic relaxation with articulated nodes						
Dynamic relaxation with friction and loose connections						
Dynamic relaxation with friction and tight connections						
Physical test, tight connections (recalibrated according to loaded nodes)					?	

Table 9 Impact of rotational stiffness of nodes on numerical and physical tests at a 1:1 scale.

Type of test	0.9 kg	1.0 kg	1.1 kg	1.2 kg	1.3 kg	1.4 kg	1.5 kg	1.6 kg
Dynamic relaxation with articulated nodes								
Dynamic relaxation with friction and loose connections								
Dynamic relaxation with friction and tight connections								



(a)



(b)

Fig. 24 By running simulations, a stress concentration (95-105 MPa) is observed in the region where the curvature is maximum (a). At 65 kg, the stress values are higher than stresses in other regions and compared to stresses with lower loads, hence the failure happens before the instability as demonstrated with the physical loading test (b).

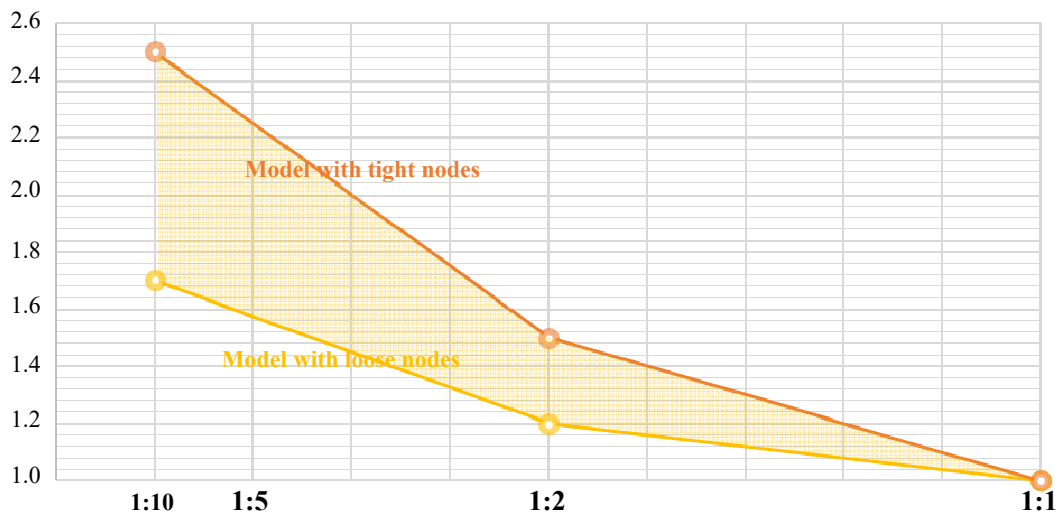


Fig. 25 First proposal for a safety factor to be applied to the result of a test on an unbraced model to take into account the non-linearity of friction and nodal stiffness, depending on the scale.

5. Conclusions and Applications

From these studies, it can be concluded that:

- For unbraced gridshell, the discrepancies between the critical buckling load obtained by the numerical method (with articulated nodes) and by the

load tests on physical scale models seem to come mainly from the rotational stiffness of the nodes.

- The contribution of the in-plane bending stiffness seems much less significant.
- These results still need to be confirmed, given the possible biases in the tests and the observed sensitivity

of the gridshell to them. We carried out about ten loading tests, which is still too small a number to correctly analyze the effect of these biases.

- Excluding experimental biases, the numerical model with articulated nodes always gives the safest value. The results extrapolated on physical models tend to overestimate the actual buckling load of the project.

- This difference decreases with the scale of the physical model (Fig. 25), the experimental biases also decrease.

- The results observed in the case of a braced gridshell are more reliable, even with small scale

models. We recommend applying to the numerical results a safety coefficient of at least 1.10 in this type of design.

- In reality, the rupture occurs earlier than numerically envisaged because of the stress generated by the deformation. We recommend applying a safety factor of at least 1.15 to the result of the dynamic relaxation to take it into account.

Thanks to this study we were also able to extrapolate the resistance of the Kagome interlaced gridshell (Fig. 26). The results, including the safety factors stated in this paper, are as follows:



Fig. 26 Load tests on the 1:10 and 1:2 physical models of the Kagome gridshell (single and double layer), and view of the scale 1 pavilion during construction.

- Single layer (asymmetric plan): 2 tests; average: 8.82 kg/m²; $s = 0.42$;

- Double layer (asymmetric plan): 2 tests; average: 12.86 kg/m²; $s = 0.33$;

- Double layer (symmetric plan): 1 test; 23.50 kg/m² according to scale 1:10 extrapolation and 28.13 kg/m² according to scale 1:2 extrapolation.

On the basis of these results, we decided to carry out the last design (symmetrical plan and double lathing).

Supplementary Materials

ELASTICA algorithm is freely available online at: <https://www.construire-l-architecture.com/07-elastica>.

Acknowledgments

The Paris City Hall and the 19th district City Hall, in

particular Sophie Godard, Cécile Becker, Eric de Grootte, Céline Belgrand, Philippe Clayette and Sylvie Roudier, for their support, as well as the inhabitants of the neighbourhood, Mr. Mayor François Dagnaud and Mrs. First Deputy Halima Jemni.

Würth France and its engineering department (Fig. 27), our main entrepreneurial partner, in particular Stephen Conord, National technical referent; and B. M. Montage of the Busson family which manufactures and gives us every year the metal pieces, and in particular Arnaud Busson.

The ENSA of Paris-la-Villette, Caroline Lecourtois, director, Vincentella De Comarmond, deputy director, Christian Brossard and Frédéric Sallet general secretary, Anne d'Orazio, President of the Board, Jérôme Candevan, accounting officer, Anaïs

Campanaud, jurist, Bruno Petit and Philippe Agricole (maintenance shop), Philippe Bourdier, in charge of student life and Marc Fayolle De Mans, Jacques Bergna and Alain Raynaud (model workshop). Yann Nussaume, Rosa de Marco and Olivier Jeudy from AMP research unit. François Guéna from MAP-MAACC laboratory.

The Paris Centrale-Supélec school, in particular Pierre Jehel and Arnaud Lafont.

Dr. Jef Rombouts, engineer and architect, and Ludovic Regnault, architect, from Bollinger + Grohmann and Dr. Bernardino D'Amico whom we contacted in 2017, and Dr. Almudena Majano Majano from the Technical University of Madrid for sharing their knowledge.

Caroline Simmenauer for the review and corrections.

Funding

This research received no external funding except Würth's furniture participation to the models at scale 1:2.

Author Contributions

Studies conducted with the participation of: ENSA-Paris-la-Villette students: Geoffrey Louison*, Mohamed Zitouni*, Anastasia Komisarova, Jose Francisco Landa, Armand Passemard, Anabel Ginesta,

Mariana Cyrino Peralva Dias, Marta Anna Mleczkowska, Léa Lallemand, Haifa Ltaïef, Miguel Madrid, Lea Carresi, Beatriz Maldonado, Gaspard Chaîne, Thibaut Morosoff, Vicente Benito Sanchis, Irene Eseverri, Marta Delgado Paez, Alejandro Mendez, Jean-Baptiste Mallard, Abderraouf Kaoula, Ana Karen Pimienta, Romain Antigny*, Tom Bardout*, Nina Bargoin, Sofia Casero, Flora Cassettari Chiaratto, Marisa De Guzman Reyes, Adrien Echeveste, Noémie Girardi*, Linus Grimminger, Ines Hitmi, Amalia Iglesias Crespo, Bryan Katekondji*, Jongmin Kim, Yeji Kim*, Antoine Maisonneuve, Hortense Majou, Ana Martin de Castro, Asnathé Mouanda, Martina Paolino, Pablo Pouget*, Alicia Tresgots*, Farah Ladhari, Mariem Ben Ali, Clotilde Burdet, Marie Gaskowiak, Élise Romagnan, Rafik Khendek, Farrah Mistoihi, Fanny de Blas*, Davy Kima, Jean Siau, Alexis Soria, Julia Tornel-Medina Matas, Julia Hladun, Alice Eising, Oriana Rey.

* Goup référent

CentraleSupélec students: Alexis Meyer, Bastien Frobert, Marc Pouyane, Louise Delahaye, Jérôme Garcia.

Conflicts of Interest

The authors declare no conflict of interest.

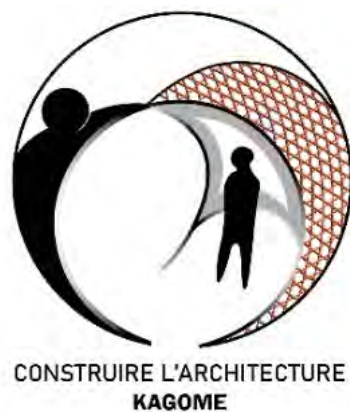


Fig. 27 Acknowledgments to our partners.

References

[1] Happold, E., and Liddell, W. 1975. "Timber Lattice Roof



for the Mannheim Bundesgartenschau." *The Structural Engineer* 53 (3): 99-135.

[2] Leyral, M., Ebode, S., Guerold, P., and Berthou, C. 2021.

- “Elastica Project: Dynamic Relaxation for Post-formed Elastic Gridshells.” In *Proceedings of the IASS Annual Symposium*, 23-27 August 2021, Surrey, U.K., pp. 1-16.
- [3] Labbé, C. 2018. “Quoi de neuf/le gridshell (des jours meilleurs)?” *Archistorm*. (in French)
- [4] Philippart de Foy, G. 1984. *Les Pygmées d'Afrique centrale*. Paris: Éditions Parenthèse. (in French)
- [5] Douthe, C. 2007. “Étude des structures élancées précontraintes en matériaux composites: application à la conception des gridshells.” Ph.D., thesis, École Nationale des Ponts et Chaussées. (in French)
- [6] Chebyshev, P. L. 1878. *Sur la coupe des vêtements*. Congrès de Paris: Association française pour l'avancement des sciences. (in French)
- [7] Boisse, P. 1994. “Modèles mécaniques et numériques pour l'analyse non-linéaire des structures minces.” Ph.D., thesis, Université de Besançon. (in French)
- [8] Bouhaya, L. 2010. “Optimisation Structurale des Gridshells.” Ph.D. thesis, École Doctorale Science Ingénierie et Environnement. (in French)
- [9] Ghys, E. 2011. “Sur la coupe des vêtements. Variation autour d'un thème de Tchebychev.” *L'Enseignement Mathématique* 57: 165-208. (in French)
- [10] Barnes, M. R. 1999. “Form Finding and Analysis of Tension Structures by Dynamic Relaxation.” *International Journal of Space Structures* 14 (2): 89-104.
- [11] Leyral, M. 2021. *Faire Tenir—Structure et architecture*, edited by de la Villette, C. Paris: Savoir Faire de L'Architecture. (in French)
- [12] Rombouts, J. 2019. “Optimal Design of Gridshells.” Ph.D. thesis, Faculty of Engineering Science of Bruxelles.

Appendix A: Numerical Modelisation by Dynamic Relaxation and ELASTICA Algorithm

Reproduced and adapted with permission from: Marc Leyral, Sylvain Ebode, Pierre Guerold, Clément Berthou; Elastica project: Dynamic Relaxation for Post-formed Elastic Gridshells, in *Inspiring the Next Generation: Proceedings of the International Conference on Spatial Structures 2020/21 (IASS2020/21-Surrey)*, edited by: Alireza Behnejad, Gerard Parke and Omidali Samavati, published by University of Surrey, Guildford, UK, in August 2021 [2].

(1) Discretization of the Chebyshev Lattice Surface

The shape resulting from the initial phase of intention, which we will now call “architect’s shape”, is not the real shape of the project, which must respect the rules of physics (especially bending). The form finding consists in determining, from the architect’s shape, what the real shape is going to be.

The first step, the division of any surface into equilateral parallelograms (a necessary condition for flat fabrication) is called a Chebyshev lattice, named after the mathematician who, in 1878, having a rather modest salary, accepted a contract to optimize the cutting of military uniforms. Chebyshev therefore devised a method to create a piece of clothing adapted to the human anatomy, in large quantities, quickly and at low cost (Fig. 1) [6].

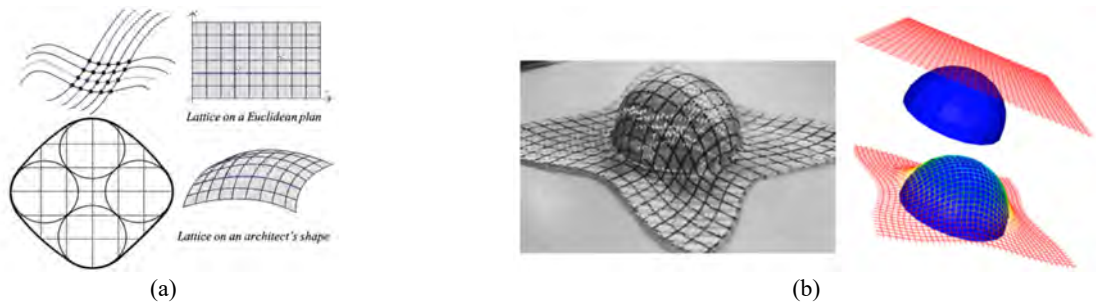


Fig. 1 (a) Discretization of a fabric and Chebyshev pattern for dressing a half-sphere [2]; (b) Chebyshev lattice: principle, by model and by dynamic relaxation (Boisse [7] and Bouhaya [8]).

The problem formulated by Ghys [9] highlights the link with gridshells: “A flattened fabric is formed by two networks of interwoven straight threads (...) which form small squares. (...) The initial small squares can become deformed: their sides do not change in length but the angle between the threads is no longer necessarily straight.” Thus, the change of angle between the threads allows them to envelop a double-curved surface without any fold. To achieve a Chebyshev lattice on any surface, one can go for a dynamic relaxation method, or by a geometric approach, called “compass method”, used by Frei Otto (Fig. 2).

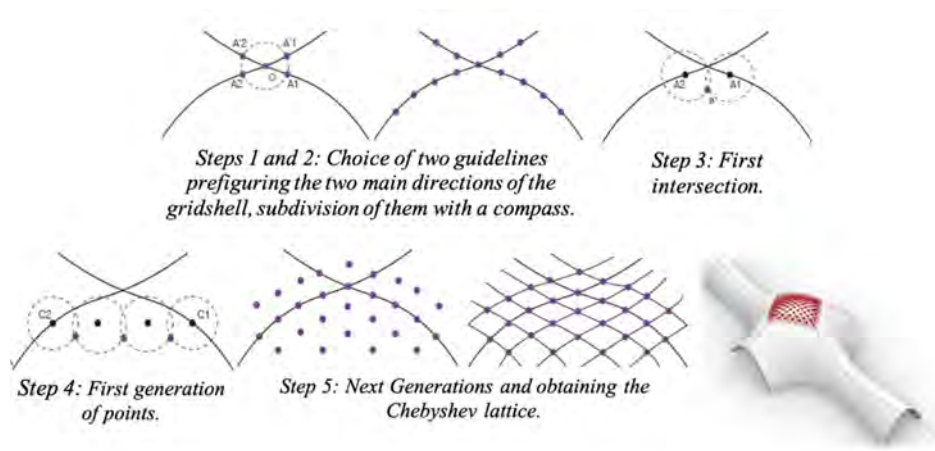


Fig. 2 Compass method and application by the ELASTICA algorithm [2].

(2) Dynamic Relaxation

This form finding method, even though simple since it is based on the laws of Newtonian physics, is iterative and heavy by its quantity of calculations (Figs. 3 and 4): its development had to wait until the end of the 20th century and computer-assisted numerical modeling. It was then applied, among others, to shells (Otter, 1964), tensioned and inflatable structures [10].

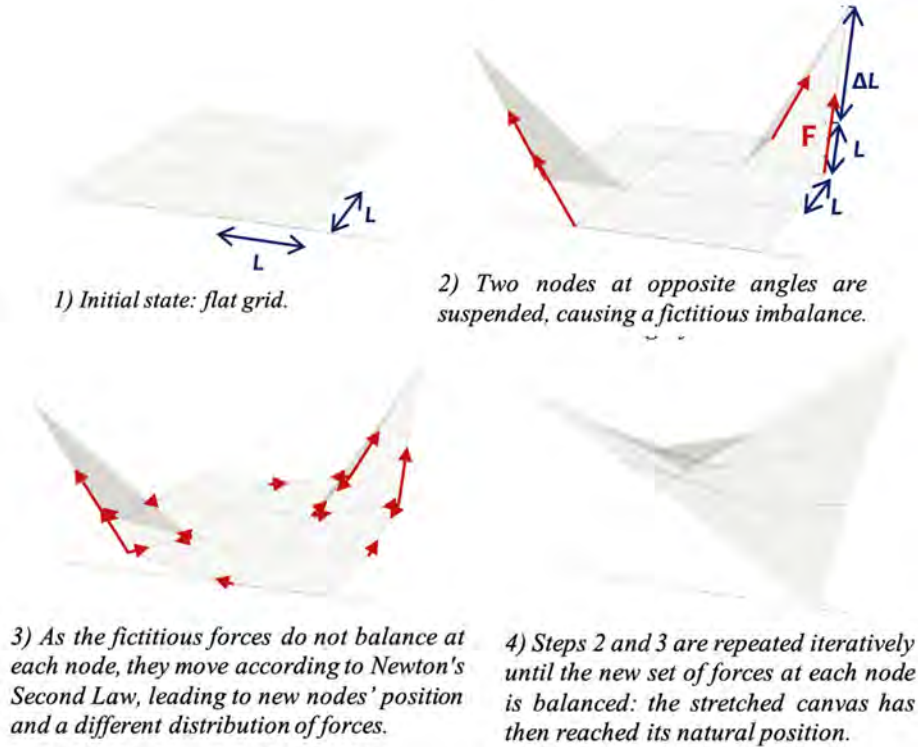


Fig. 3 General principle of dynamic relaxation applied to an example of the form finding of a stretched canvas [11].

Dynamic relaxation allows solving static equilibrium problems by a fictitious and iterative dynamic calculation. It is valid for large deflections. According to Barnes [10], “the basis of the method is to trace step-by-step for small time increments, Δt , the motion of each node of a structure (from an initial disturbed instant) until, due to artificial damping, the structure comes to rest in static equilibrium.”

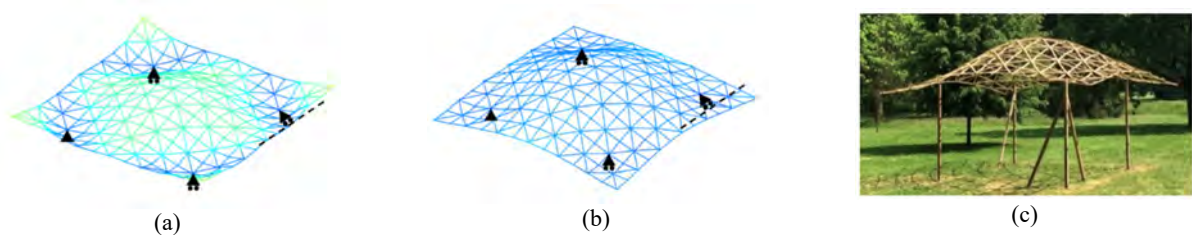


Fig. 4 Trial gridshell by Rombouts [12]: mesh of the architect's form (a), form finding after dynamic relaxation (b), and built project (c).

(3) Theory from an Analytical Point of View

The architect's shape is not the natural form of the project, so it is not at rest. It wants to move to its natural position: it needs to relax. Thus, the fictitious motion of a structure modeled by a discrete mesh of bars (for a gridshell, this comes from a Chebyshev lattice, it therefore represents the real physical elements of the structure), at the intersection of which are located the nodes subjected to forces, must be calculated. Indeed, according to Newton's second law $\sum \vec{F} = m * \vec{a}$, if the forces at each node do not balance, then the nodes (to which we attribute a mass, real or fictitious) experience a fictitious acceleration $\vec{a} = \sum \vec{F} / m$, and therefore move

at a velocity that varies with time. This lets us calculate at each iteration, the position of each node at the next instant.

In the case of a gridshell, there are (at least) three forces acting at the nodes (Fig. 5): the nodal dead weight ($\vec{F} = \mathbf{m} * \vec{g}$), the force induced by the bending of the elements as described by Barnes, and the Hooke force in each element, proportional to their axial stiffness and deformation ($\vec{F} = \mathbf{EA} * \Delta\mathbf{L}/\mathbf{L}$), which ensures the equilibrium of each node. To calculate the value of the bending forces, let us start from the bending moment M which causes the bending of the elements, the force field applied to the nodes is deduced from the relation $\vec{M} = \vec{OA} \wedge \vec{F}$. The algebraic value of the moment being $M = \frac{EI}{R}$ and, by definition, $R = \frac{L_{i-1,i+1}}{2 \sin(\alpha_i)}$, we obtain

$$\mathbf{M} = \frac{2EI \sin(\alpha_i)}{L_{i-1,i+1}}$$

We deduce that in a system composed of curved beams, each trio of consecutive nodes admits on the ends of each of the two segments formed two opposite forces of the same values, $F_{i-1,i} = \frac{2EI \sin(\alpha_i)}{L_{i-1,i} * L_{i-1,i+1}}$ for the first segment and $F_{i,i+1} = \frac{2EI \sin(\alpha_i)}{L_{i,i+1} * L_{i-1,i+1}}$ for the second.

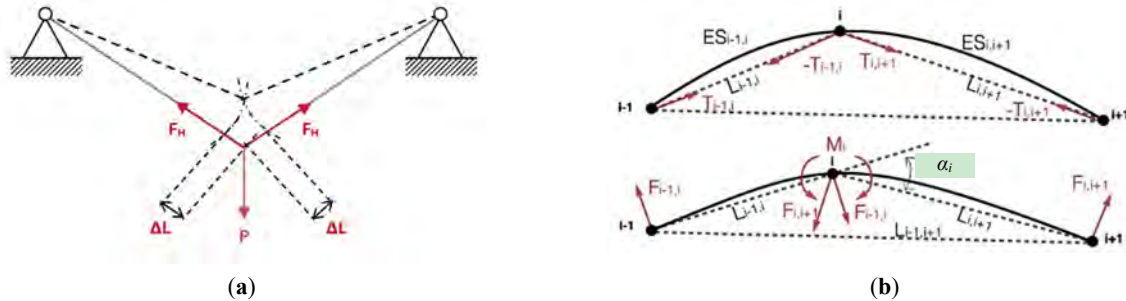


Fig. 5 Equilibrium of a node by the spring forces from Hooke’s law on the example of a loaded cable (a), and forces due to bending in the case of a gridshell (b).

Once the acceleration \vec{a}_t at a fictitious instant t has been calculated and knowing the initial velocities \vec{v}_{t+dt} at the same instant, we deduce nodal velocities at the following instant $t + dt$:

$$D = \vec{v}_{t+\frac{dt}{2}} * dt = \vec{a}_t * \frac{dt^2}{2} + \vec{v}_t * dt \tag{5}$$

We then obtain the positions of each node at time $t + dt$. The operation is repeated until an equilibrium of forces is reached at each node: the structure is then at its natural position. This can only be done by adding a damping in the system, which is explained below.

(4) General Theory from an Energetic Point of View

At the initial instant, the deviation between the initial architect’s shape and the equilibrium shape being maximum, the potential energy of the system is maximum, the initial nodal velocities being zero, the kinetic energy $\sum_{nodes} \frac{1}{2} * \mathbf{m} * \mathbf{v}^2$ of the system is as well. The relaxation then causes the nodes to move: the structure is going closer to its equilibrium, the potential energy is reduced by conversion into kinetic energy. When the system passes through its equilibrium position, the forces balance and the potential energy becomes zero. But nodal velocities, which are then maximum (and therefore the kinetic energy as well), cause a continuation of the movement in the opposite direction: the system oscillates.

At convergence, which can only be reached by adding damping to dissipate the total energy of the system, equilibrium position is obtained when the potential energy is zero (the forces are in equilibrium) and the kinetic energy is zero (the nodes no longer move: their velocities is zero), see Fig. 6.

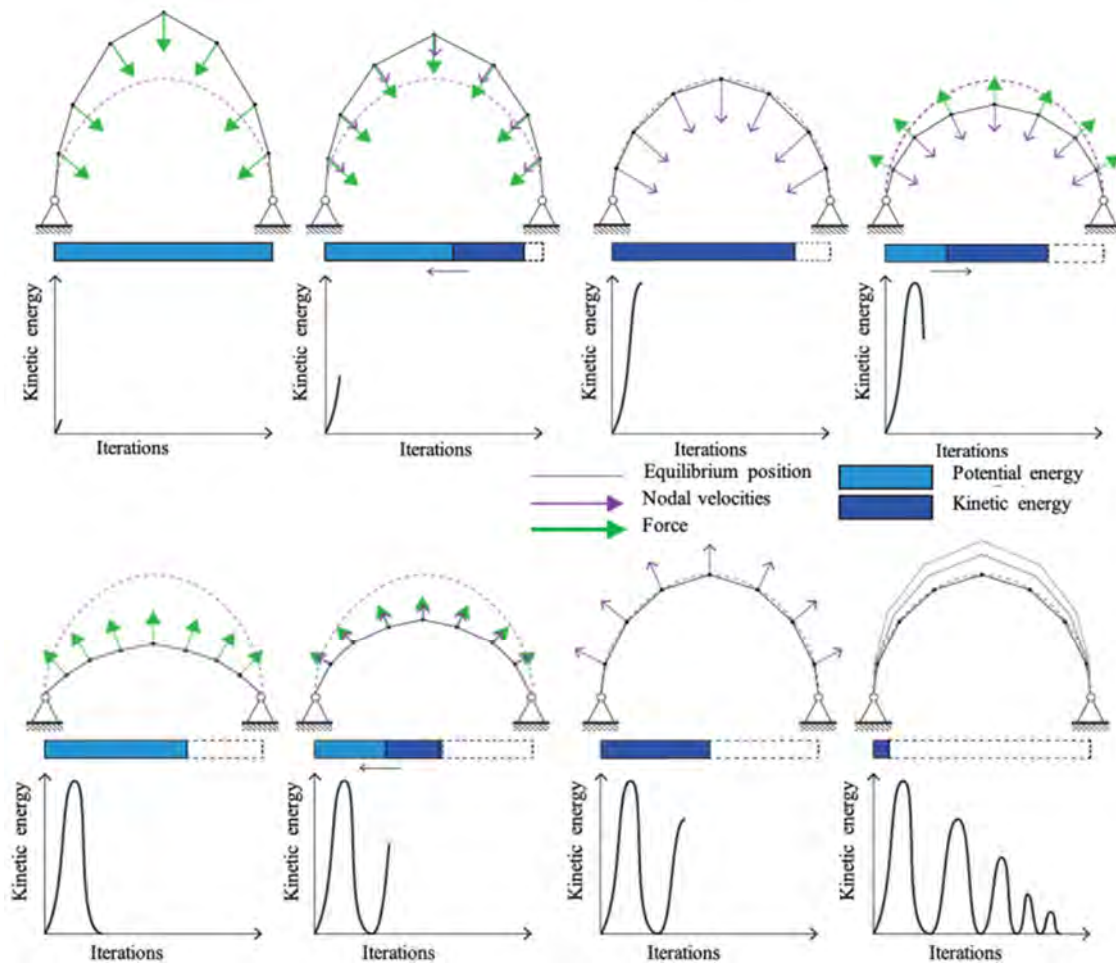


Fig. 6 Energy transfer during the dynamic relaxation of a gridshell [2].

Damping can be either viscous damping by the addition of an additional force $\vec{F}_a = -c * \vec{v}$ or kinetic damping. Our ELASTICA algorithm uses this last method because it does not require setting new parameters and often allows for faster convergence. Barnes [10] explains that kinetic damping “is an artificial damping (...). In this procedure the undamped motion of the structure is traced and when a local peak in the total kinetic energy of the system is detected, all velocity components are set to zero. The process is then restarted from the current geometry and repeated through further (generally decreasing) peaks until the energy of all modes of vibration has been dissipated and static equilibrium is achieved.”

(5) Calculation of the Time Interval dt of the Iterations

A time interval too short or a nodal mass too high can lead to a divergence. Commonly, we choose a time interval dt and deduce from it the fictitious nodal masses—different from the real nodal masses of the project—able to ensure the convergence of the algorithm by the Barnes-Han-Lee formula: $m = \frac{dt^2}{2} * (\sum_{\mu} R_a + \sum_{\mu} R_f)$ where μ is the number of bars connected to each node (4 without bracing and 6 with). For convenience, we have set in ELASTICA tool the nodal mass m equal to the real mass and deducted dt . This simple formula does not always ensure convergence: it is advisable to divide it by a safety factor (1.2 has been chosen in our case after several tests).

(6) The ELASTICA Algorithm

This algorithm is the concrete application of the above, usable for any type of elastic gridshell, and available in open source on the website: www.construire-l-architecture.com (Fig. 7).

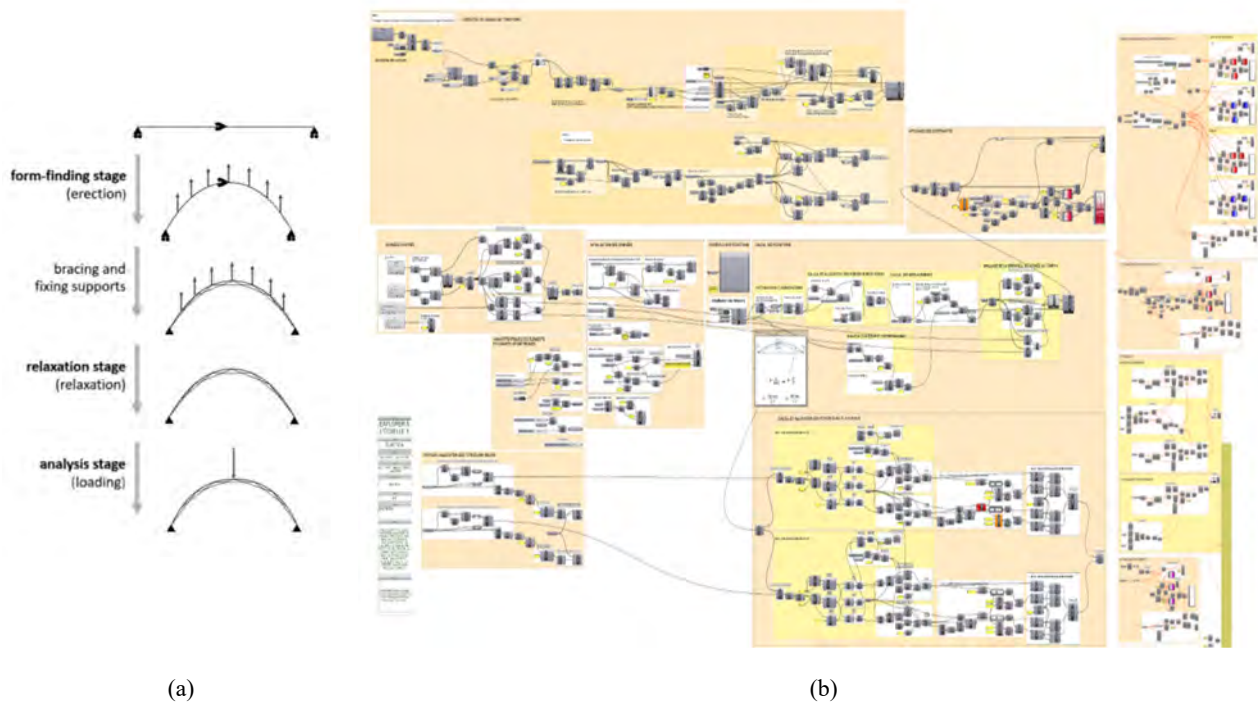


Fig. 7 Chronology of form finding stages and stability control using dynamic relaxation by Rombouts [12], and extract of the ELASTICA algorithm [2].

The ELASTICA algorithm is able to:

- Divide any surface into a Chebyshev network using the compass method.
- Solve form finding according to different parameters (geometry, single or double layering, with or without bracing, with or without shear blocks, etc.).
- Find the critical load that will cause the buckling of the structure.
- Give stress in timber lattices.
- Give stress in metallic or timber bracing elements.
- Verify the local non-buckling condition of every bar in the project.
- Calculate horizontal reactions.
- Automatically draw up the fabrication and assembly plans of the structure.